Microelectronic Engineering 185–186 (2018) 43–47

Contents lists available at ScienceDirect

Microelectronic Engineering

journal homepage: www.elsevier.com/locate/mee

Research paper

Spike-timing-dependent plasticity of polyaniline-based memristive element

D.A. Lapkin [a,b], A.V. Emelyanov [a,b,*], V.A. Demin [a,b], T.S. Berzina [c], V.V. Erokhin [a,c]

[a] National Research Center, Kurchatov Institute, 123182 Moscow, Russia
[b] Moscow Institute of Physics and Technology (State University), 141700 Dolgoprudny, Moscow Region, Russia
[c] CNR-IMEM (National Research Council, Institute of Materials for Electronics and Magnetism), Parco Area delle Scienze, 37A, 43124 Parma, Italy

ARTICLE INFO

Article history:
Received 31 May 2017
Received in revised form 12 September 2017
Accepted 30 October 2017
Available online 31 October 2017

Keywords:
Memristor
Resistive switching
Spike-timing-dependent plasticity
Artificial neural networks
Polyaniline

ABSTRACT

A phenomenological model of the polyaniline (PANI) based memristive element's conductivity evolution during the application of varying voltages is presented in this work. The model is based on the experimental data on the conductance versus time dependencies for a set of applied voltages. The model could be used for simulation of complex artificial neural networks (ANNs) based on PANI memristive elements. We have experimentally shown that organic PANI-based memristive element could be trained by the biologically inspired spike-timing-dependent plasticity mechanism. The results obtained by the simulation using the developed model are in a good agreement with the experimental data. It allows considering the usage of the organic memristive element as a synaptic element in a hardware realization of spiking ANNs capable of non-supervised learning.

1. Introduction

In natural neural systems, neurons communicate with each other with action potential pulses – spikes [1]. In comparison with it, conventional (formal) ANNs have, at the most, biologically implausible principles of work, such as a stationary activation function, pure mathematical weight update algorithms, non-dynamical functioning (clock by clock and layer by layer). Moreover, the pulsed neural networks implemented in hardware have significantly reduced power consumption [2]. Therefore, the development of spiking neuromorphic hardware circuits, which explicitly mimic neural spikes, is of high interest. In the simplest spiking neuromorphic networks, each neuron is represented as a leaky-integrate-and-fire unit, which integrates incoming spikes and fires its own spike when the integrated action potential reaches a certain threshold [1]. The fired spike, weighted according to the strengths of the corresponding synapses, is applied to the input of other neurons. Additionally, the fired spike is also propagated backward to the input synapses to provide their weights adaptation – for example, according to the spike-timing-dependent-plasticity (STDP) rule [3], which ensures Hebbian learning [4]. In the simplest case of a synaptic connection between two excitatory neurons, its strength changes if the spikes from pre- and post-synaptic neurons come with a small correlated difference in time. When the postsynaptic spike comes just after the presynaptic one, the order is considered correct (indicating a causal relationship) and the synaptic strength is enhanced. Otherwise, the order is erroneous (indicating an anti-causal relationship) and the strength is weakened [5].

The STDP mechanism was shown to emerge naturally in memristive elements [6] prospective for a hardware realization of ANNs. Originally, the memristor was suggested in 1971 as a passive element, establishing the relation between magnetic flux and electric charge [7], but recently it is considered to be an element with resistive switching properties controlled by applied voltage [8,9]. There were developed a lot of materials showing memristive behavior including oxides [10–13], amorphous silicon [14], other inorganic [15,16] and organic [17–20] materials. The last are of great interest caused by well-developed methods of preparation and formation of polymers [21], their flexibility, biocompatibility and low cost. Memristive elements based on PANI have demonstrated good characteristics in synaptic-mimicking operations in simple ANNs [22,23].

STDP behavior was shown in organic memristive element based on PEDOT:PSS [24,25]. However, used shapes of applied voltages and the respective response caused by the STDP mechanism were not biologically plausible and the question of applicability of such dependence for the ANN training is still open.

Thus, the main goal of this work was to show that organic PANI-based memristive element could be trained by the biologically inspired STDP mechanism. We have also developed a phenomenological model

* Corresponding author at: National Research Center, Kurchatov Institute, 123182 Moscow, Russia.
E-mail addresses: lapkin@phystech.edu (D.A. Lapkin), av.emelyanov@physics.msu.ru (A.V. Emelyanov).

https://doi.org/10.1016/j.mee.2017.10.017
0167-9317/

of resistive state evolution during the application of a varying voltage. It allows also to use the model for simulation of complex hardware ANNs capable of non-supervised learning based on PANI memristive elements.

2. Materials and methods

PANI-based memristive elements were fabricated following the technique reported in [26]. A solution of PANI (Mw ≈ 100,000, Sigma Aldrich) was prepared with a concentration of 0.1 mg/ml in 1-methyl-2-pyrrolidone (Sigma Aldrich ACS reagent ≥99.0%) with the addition of 10% of Toluene (AnalaR NORMAPUR® ACS). This solution was filtered twice and then deposited by Langmuir–Schaefer technique onto a glass substrate (1.5×0.5 cm^2) with two Cr or Ti electrodes. The PANI conductive channel was formed by depositing 60 layers of the polymer in its emeraldine base form and then transforming it into the emeraldine salt conducting form by a doping process in HCl vapor for 2 min. Subsequently, a stripe of solid electrolyte (about 1 mm width restricted by Kapton stripes) was deposited in the center of the PANI channel in a crossed configuration and a silver wire (with a diameter of 0.05 mm), inserted in the polyelectrolyte, worked as a reference electrode. The electrolyte was prepared by addition of polyethylene oxide (PEO, Sigma Aldrich) with a molecular weight of $8 \cdot 10^6$ Da (30 mg/ml) in a water solution of $LiClO_4$ (0.1 M, Sigma Aldrich). The final structure was additionally doped in HCl vapor and covered by Kapton film. The covering Kapton film significantly reduces the out effusion of doping Cl^- ions from the PANI film. As a result the life-time of PANI-based memristive devices increases up to several months of operation. The voltage pulses application and the current measurements were performed by means of a Keithley 4200-SCS Semiconductor Characterization System.

3. Results and discussion

3.1. Memristive element

The electrophysical characterization was performed as described elsewhere [26]. Silver wire (called "gate" by the analogy to field effect transistors) and one of the electrodes on the substrate ("drain") were grounded through ammeters, whereas voltage was applied to another electrode on the substrate ("source") as shown in Fig. 1a. The I–V curves were measured by scanning voltage upwards from 0 to +1 V, then downwards to −1 V and then back to 0 V with a step of 0.1 V. For each step, the current value was measured after 60 s delay of the voltage application. This time delay value was found to be an optimal one for studying cyclic characteristics of PANI-based organic memristive elements. Resulting curves for the total current (through the "source" electrode) and for the ionic current (through the silver "gate" electrode) are shown in Fig. 1b and in inset respectively.

The total current increases drastically during the upward scan when the applied voltage is above +0.4 V due to the oxidation of PANI channel with a respective positive peak in the ionic current. When the voltage decreases to +0.1 V the total current readily drops due to the PANI reduction that is characterized by the appearance of the negative peak in the ionic current. The conductance of the memristor remains low within further voltage scanning in negative values since the PANI channel is reduced. Such hysteretic behavior and preservation of resistance in the range of voltages between +0.1 and +0.4 V allow considering these memristive elements as good candidates for the STDP learning. The properties of the elements are rather stable for at least 50 first cycles [27]. It should be noted that we have not observed any significant difference between the characteristics of the elements with Cr and Ti electrodes.

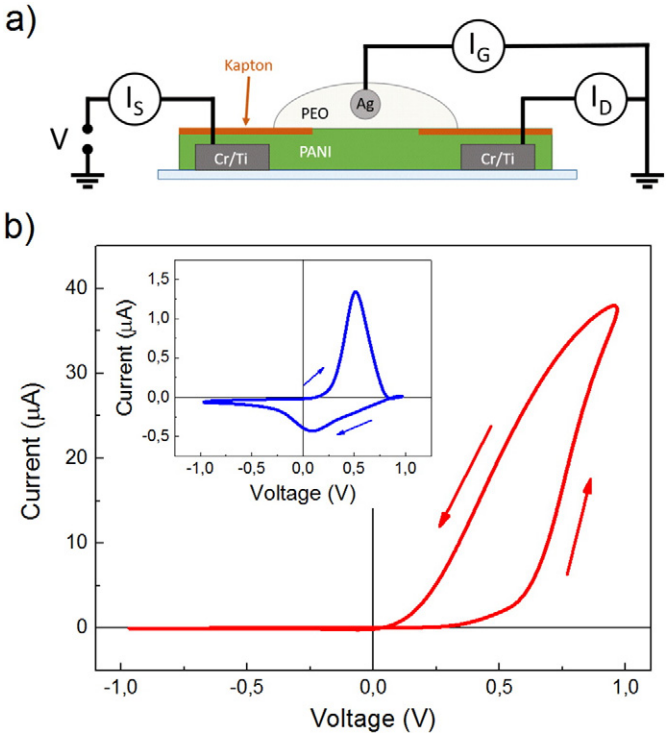

Fig. 1. Schematic representation of the PANI-based memristive element (a) and the voltage-current characteristics of the element (inset – the ionic current through the Ag wire) (b).

3.2. Resistive switching kinetics

In order to carry out the experiment on the STDP response measurement in a PANI-based organic memristive element, one has to establish the shapes of voltage pulses appropriate for changes of the resistance state within spikes and preservation of its state between them. We have chosen a triangular symmetric pulse shape as it was shown to cause the response similar to the biological one [28], but the amplitude and the length of the pulses had to be established by memristive elements characteristics. Despite the intense investigation of the resistive switching properties of PANI-based memristive elements was performed [29,30], the detailed information on the resistive switching kinetics (speeds) on the applied voltage is not available. Conductance-time dependencies of our element under a specific applied voltage could not be obtained analytically from the first principles due to complicated potential distribution in the PANI active zone. Experimental data for two voltages, potentiating and depressing, could be fitted by biexponents [31], but the dependence of characteristic times of resistive switching on the applied voltage is unknown. The published model [32] describes the ion migration through the PEO/PANI interface and electrochemical redox reactions occurring on the Ag wire as well as in the PANI channel during the operation of the element. It is based on the numerical solution of a system of the Butler-Volmer differential equations for various points along the active zone of the PANI channel. Consequently, one can assume that the full conductance depends on the time and the applied voltage similarly to the Butler-Volmer activation character. In this section we investigate the dependence of resistive switching kinetics on the applied voltage value.

As the conductance of the PANI-based memristive element tends to increase under applied voltage more than +0.4 V, we used voltages in the range of +0.6 to +0.8 V for the potentiation kinetics measurements. Otherwise, the conductance decreases under the voltage less than +0.1 V and for the depression kinetics measurements we used voltages in the range of −0.3 to −0.1 V. Before each measurement, conductance of the memristive element was reset to the maximum value

for the depression and to the minimum one for the potentiation by the appropriate voltage value application. Typical experimentally measured dependencies are shown in Fig. 2a.

Obtained kinetics could be fitted by the following system:

$$G(t) = \begin{cases} G_{max} - (G_{max} - G_{min}) \cdot \exp(-\frac{t}{\tau_p(V)}), \text{if } V > 0.4 \\ G_{min} + (G_{max} - G_{min}) \cdot \exp(\frac{t}{\tau_d(V)}), \text{if } V < 0.1 \end{cases},$$

where G_{max} and G_{min} are maximum and minimum values of the conductivity, τ_p and τ_d – characteristic times of the potentiation and depression respectively.

The conductivity values depend on the geometry of the sample and typically the minimum one is equal to 10^{-6} S and the maximum is about 10^{-5} S. Characteristic times tend to decrease with increasing absolute values of the applied voltage, what is clearly visible from the dependencies of inverse characteristic times on applied voltages shown in Fig. 2b and c. The linear dependencies are in a good agreement with the predictions given by Butler-Volmer equations. Thus, typical empirical laws for characteristic times are $\tau_d(V) = {}^{2.8}/_{(0.1-V)}$ for the depression and $\tau_p(V) = {}^{26}/_{(V-0.4)}$ for the potentiation. The values in the denominator are determined by the PANI redox potential, while the values in the numerator depend on the geometry of the sample and vary from sample to sample. The main feature is the fact that the characteristic time for the depression always is much lower than that for the potentiation (in absolute agreement with all available experimental data). This phenomenological model could be used for simulation of the time evolution of the organic memristive element's conductive state during application of varying voltages.

3.3. Spike-timing-dependent plasticity

For the STDP implementation, the connected gate and drain electrodes were assigned as a presynaptic input and the source electrode was a postsynaptic one. We used identical potential pulses as pre- and postsynaptic spikes, but applied constant bias voltage +0.2 V to avoid changes in conductivity between spikes conditioned by the value of the PANI redox equilibrium potential. Amplitudes of the spikes were chosen to be 0.3 V, so the maximum voltage drop across a memristive element was equal to +0.8 V and the minimum one was equal to −0.4 V, which is within working range of the PANI-based memristive element. The characteristic times of conductance variation were taken into account when choosing durations of the pulses to be sufficient for the conductivity changes. Full length of the pulse was 800 s, a half of this time the potential increased from 0 to +0.3 V and the remaining time the potential increased from −0.3 to 0 V. Postsynaptic pulses were applied after presynaptic pulses in a delay time Δt, that could be also a negative one. Actually, the interchange of pre- and postsynaptic electrodes changes only the sign of the delay Δt values. Resulting pulses form and the definition of Δt are shown in Fig. 3a. Full voltage (the difference between post- and pre-synaptic potentials) across the memristive element during the measurement for the delay time $\Delta t = 200$ s is shown in Fig. 3b.

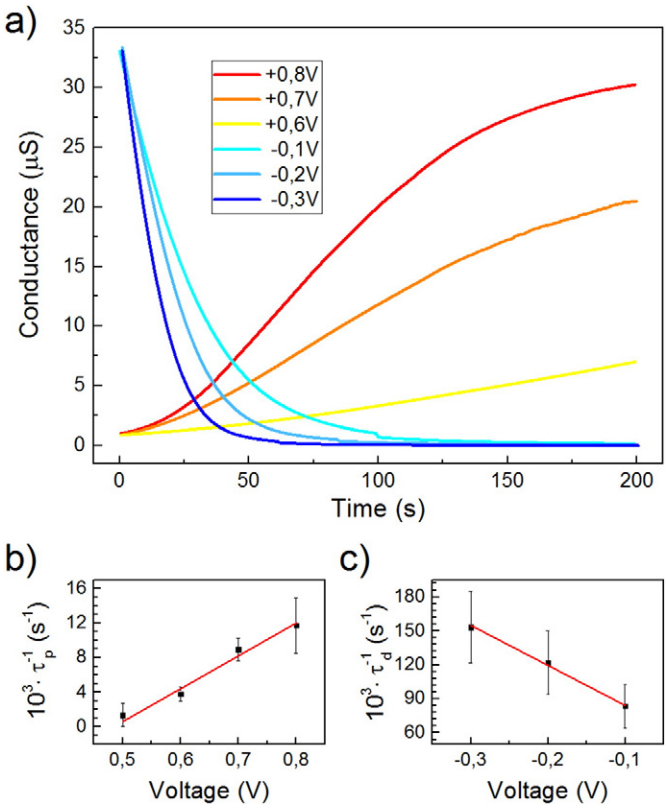

Fig. 2. Typical kinetics of the memristive elements conductivity variations under different applied voltages (a) and the inverse characteristic time dependence on the applied voltages for the potentiation (b) and depression (c).

Conductances were measured by the application of the testing voltage of +0.3 V within 30 s before and after the pre- and postsynaptic pulses sequence. Generally, in neuromorphic applications of memristive elements, synaptic weights are equal to their conductance. Thus, weight changes were considered as $\frac{G_{fin} - G_{ini}}{G_{ini}}$, where G_{fin} and G_{ini} are the final and initial conductances respectively. We measured weight changes due to the STDP for $\Delta t = \pm 1000, \pm 600, \pm 400, \pm 200$ and ± 100 s, each time resetting conductance value before the application of spikes. Thus determined weight change dependence on delay time (STDP window) averaged over several samples is shown in Fig. 4. On the base of the phenomenological memristive element kinetic model described above, we have simulated the application of the same voltage pulses for the selected delay times and the result is also shown in Fig. 4.

The weight change decreases monotonically with the increasing delay time and a jump from negative to positive values occurs at the delay time of 0 s. Depression for the both longest Δt, negative and positive, can be explained by the following reason. In this case, the same absolute values of the potential versus equilibrium potential +0.2 V, but with opposite sign, were applied to the memristive element for the same time, but, as it was shown above, the characteristic time of the depression is less than that for the potentiation. Then applying the voltages with the same amplitude (versus equilibrium potential) for the same time would likely decrease the conductivity of organic memristive device than increase it. The same reason caused less weight change for the positive Δt values than that for the negative ones. The results of the simulation demonstrate the qualitatively similar behavior and the quantitative estimations of the conductance change are within the limits of experimental error (Fig. 4). It should be also noted, that conductance retention time of the PANI-based memristive devices under equilibrium potential is about 24 h long. It is not enough for practical use but it could be elongated i) instrumentally, by periodical monitoring and correction of resistive state, ii) synthetically, by optimization of composition of polymer materials used in this work, e.g. by adding of metallic nanoparticles in PANI layer [33].

Of course, from the practical point of view, the characteristic switching times of PANI-based memristors should be reduced. There are some promising efforts on the way to reach this goal such as a decrease of the active PANI film thickness down to a few molecular layers and optimization of chemical and electrical properties of electrolyte used in a memristive element.

4. Conclusions

In conclusion, we have experimentally demonstrated that the resistive state of the PANI-based memristive element could be tuned by the STDP mechanism. The experimental STDP window is in a good

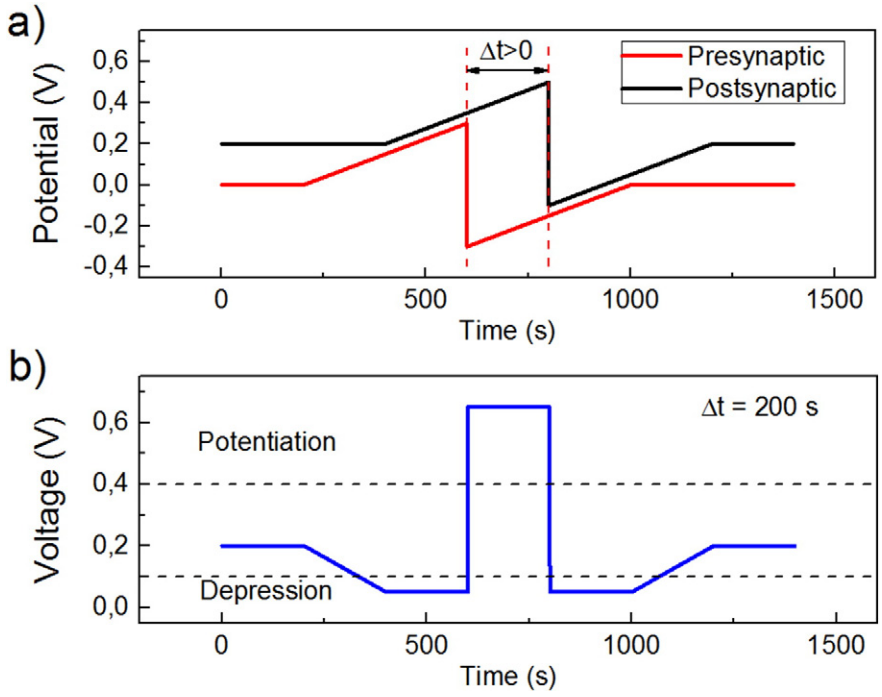

Fig. 3. a) Shapes of presynaptic (black line) and postsynaptic (red) potential pulses. b) Resulting voltage across the memristive element for the specific Δt = 200 s value.

agreement with the data available for the biological synapses [5] and could provide a basis for unsupervised learning [34]. Simulation results show the consistency of the proposed memristive element kinetic model and these results could be further used for the simulation of the hardware realization of spiking ANNs based on organic memristive elements as synapses.

Acknowledgments

The work was partially supported by the Russian Science Foundation (16-13-00052). Measurements were carried out on the equipment of the Resource center of electrophysical methods (Complex of NBICS-technologies of Kurchatov Institute).

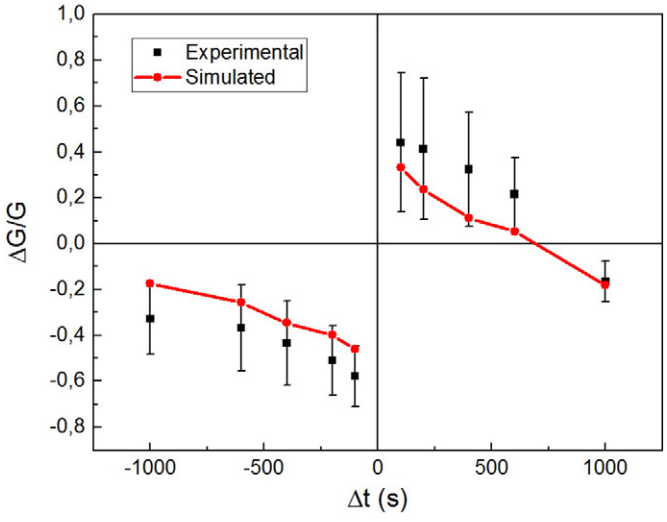

Fig. 4. STDP window for the organic PANI-based memristive element – relative weight (conductance) changes for different delay Δt values: experimentally obtained (black squares) and simulated (red circles and lines).

References

[1] W. Gerstner, W. Kistler, Spiking Neuron Models, Cambridge U. Press, New York, NY, 2008.
[2] P. Merolla, J. Arthur, F. Akopyan, N. Imam, R. Manohar, D.S. Modha, A digital neurosynaptic core using embedded crossbar memory with 45 pJ per spike in 45 nm, 2011 IEEE Custom Integrated Circuits Conference (CICC) 2011, pp. 1–4, https://doi.org/10.1109/CICC.2011.6055294.
[3] N. Caporale, Y. Dan, Spike timing–dependent plasticity: a Hebbian learning rule, Annu. Rev. Neurosci. 31 (2008) 25–46, https://doi.org/10.1146/anrnurev.neuro.31.060407.125639.
[4] D.O. Hebb, The Organization of Behavior, Wiley & Sons, New York, NY, 1949.
[5] G.Q. Bi, M.M. Poo, Synaptic modifications in cultured hippocampal neurons: dependence on spike timing, synaptic strength, and postsynaptic cell type, J. Neurosci. 18 (24) (15 December 1998) 10464–10472.
[6] B. Linares-Barranco, T. Serrano-Gotarredona, Memristance can explain spike-time-dependent-plasticity in neural synapses, Nat. Precedings 1 (2009) 2009.
[7] L. Chua, Memristor-the missing circuit element, IEEE Trans. Circuit Theory 18 (5) (1971) 507–519, https://doi.org/10.1109/TCT.1971.1083337.
[8] S. Vongehr, X. Meng, The missing memristor has not been found, Sci Rep 5 (2015)https://doi.org/10.1038/srep11657.
[9] V.A. Demin, V.V. Erokhin, Hidden symmetry shows what a memristor is, Int. J. Unconv. Comput. 12 (5–6) (2016) 433–438.
[10] D.B. Strukov, G.S. Snider, D.R. Stewart, R.S. Williams, The missing memristor found, Nature 453 (7191) (2008) 80–83, https://doi.org/10.1038/nature06932.
[11] A.N. Mikhaylov, A.I. Belov, D.V. Guseinov, D.S. Korolev, I.N. Antonov, D.V. Efimovykh, ... A.I. Bobrov, Bipolar resistive switching and charge transport in silicon oxide memristor, Mater. Sci. Eng. B 194 (2015) 48–54, https://doi.org/10.1016/jr.mseb.2014.12.029.
[12] A.C. Torrezan, J.P. Strachan, G. Medeiros-Ribeiro, R.S. Williams, Sub-nanosecond switching of a tantalum oxide memristor, Nanotechnology 22 (48) (2011), 485203. https://doi.org/10.1088/0957-4484/22/48/485203.
[13] S. Kumar, Z. Wang, X. Huang, N. Kumari, N. Davila, J.P. Strachan, ... R.S. Williams, Oxygen migration during resistance switching and failure of hafnium oxide memristors, Appl. Phys. Lett. 110 (10) (2017) 103503, https://doi.org/10.1063/1.4974535.
[14] S.H. Jo, K.H. Kim, W. Lu, High-density crossbar arrays based on a Si memristive system, Nano Lett. 9 (2) (2009) 870–874, https://doi.org/10.1021/nl8037689.
[15] H. Nili, T. Ahmed, S. Walia, R. Ramanathan, A.E. Kandjani, S. Rubanov, ... S. Sriram, Microstructure and dynamics of vacancy-induced nanofilamentary switching network in donor doped SrTiO3 − x memristors, Nanotechnology 27 (50) (2016) 505210, https://doi.org/10.1088/0957-4484/27/50/505210.
[16] S. Wang, W. Wang, C. Yakopcic, E. Shin, G. Subramanyam, T.M. Taha, Experimental study of LiNbO3 memristors for use in neuromorphic computing, Microelectron. Eng. 168 (2017) 37–40, https://doi.org/10.1016/j.mee.2016.10.007.
[17] V. Erokhin, T. Berzina, M.P. Fontana, Hybrid electronic device based on polyaniline-polyethyleneoxide junction, J. Appl. Phys. 97 (6) (2005), 064501. https://doi.org/10.1063/1.1861508.

[18] B.C. Das, R.G. Pillai, Y. Wu, R.L. McCreery, Redox-gated three-terminal organic memory devices: effect of composition and environment on performance, ACS Appl. Mater. Interfaces 5 (21) (2013) 11052–11058, https://doi.org/10.1021/am4032828.
[19] B. Sun, X. Zhang, G. Zhou, P. Li, Y. Zhang, H. Wang, ... Y. Zhao, An organic nonvolatile resistive switching memory device fabricated with natural pectin from fruit peel, Org. Electron. 42 (2017) 181–186, https://doi.org/10.1016/j.orgel.2016.12.037.
[20] Y. van de Burgt, E. Lubberman, E.J. Fuller, S.T. Keene, G.C. Faria, S. Agarwal, ... A. Salleo, A non-volatile organic electrochemical device as a low-voltage artificial synapse for neuromorphic computing, Nat. Mater. 16 (4) (2017) 414–418, https://doi.org/10.1038/nmat4856.
[21] D.A. Lapkin, A.N. Korovin, V.A. Demin, A.V. Emelyanov, S.N. Chvalun, Organic memristive device based on polyaniline film prepared by spin coating, Bio. Nano Sci. 5 (3) (2015) 181–184, https://doi.org/10.1007/s12668-015-0177-6.
[22] V.A. Demin, V.V. Erokhin, A.V. Emelyanov, S. Battistoni, G. Baldi, S. Iannotta, P.K. Kashkarov, M.V. Kovalchuk, Hardware elementary perceptron based on polyaniline memristive devices, Org. Electron. 25 (2015) 16–20, https://doi.org/10.1016/j.orgel.2015.06.015.
[23] A.V. Emelyanov, D.A. Lapkin, V.A. Demin, V.V. Erokhin, S. Battistoni, G. Baldi, A. Dimonte, A.N. Korovin, S. Iannotta, P.K. Kashkarov, M.V. Kovalchuk, First steps towards the realization of a double layer perceptron based on organic memristive devices, AIP Adv. 6 (2016), 111301. https://doi.org/10.1063/1.4966257.
[24] Fei Zeng, et al., Learning processes modulated by the interface effects in a Ti/conducting polymer/Ti resistive switching cell, RSC Adv. (2014) 14822–14828 4.29 https://doi.org/10.1039/C3RA46679E.
[25] Sizhao Li, et al., Synaptic plasticity and learning behaviours mimicked through Ag interface movement in an Ag/conducting polymer/Ta memristive system, J. Mater. Chem. (2013) 5292–5298 C 1.34 https://doi.org/10.1039/C3TC30575A.
[26] V. Erokhin, T. Berzina, P. Camorani, A. Smerieri, D. Vavoulis, J. Feng, M.P. Fontana, Material memristive device circuits with synaptic plasticity: learning and memory, Bio. Nano Sci. 1 (1–2) (2011) 24–30, https://doi.org/10.1007/2Fs12668-011-0004-7.
[27] V. Erokhin, T. Berzina, P. Camorani, M.P. Fontana, On the stability of polymeric electrochemical elements for adaptive networks, Colloids Surf. A Physicochem. Eng. Asp. 321 (1) (2008) 218–221, https://doi.org/10.1016/j.colsurfa.2008.02.040.
[28] S. Saïghi, C.G. Mayr, T. Serrano-Gotarredona, H. Schmidt, G. Lecerf, J. Tomas, ... S. La Barbera, Plasticity in memristive devices for spiking neural networks, Front. Neurosci. 9 (2015) 51, https://doi.org/10.3389/fnins.2015.00051.
[29] T. Berzina, S. Erokhina, P. Camorani, O. Konovalov, V. Erokhin, M.P. Fontana, Electrochemical control of the conductivity in an organic memristor: a time-resolved X-ray fluorescence study of ionic drift as a function of the applied voltage, ACS Appl. Mater. Interfaces 1 (10) (2009) 2115–2118, https://doi.org/10.1021/am900464k.
[30] S. Battistoni, A. Dimonte, V. Erokhin, Spectrophotometric characterization of organic memristive devices, Org. Electron. 38 (2016) 79–83, https://doi.org/10.1016/j.orgel.2016.08.004.
[31] V. Allodi, V. Erokhin, M.P. Fontana, Effect of temperature on the electrical properties of an organic memristive device, J. Appl. Phys. 108 (7) (2010), 074510. https://doi.org/10.1063/1.3484038.
[32] V.A. Demin, V.V. Erokhin, P.K. Kashkarov, M.V. Kovalchuk, Electrochemical model of the polyaniline based organic memristive device, J. Appl. Phys. 116 (6) (2014), 064507. https://doi.org/10.1063/1.4893022.
[33] V. Erokhin, T. Berzina, K. Gorshkov, P. Camorani, A. Pucci, L. Ricci, G. Ruggeri, R. Sigala, A. Shuz, Stochastic hybrid 3D matrix: learning and adaptation of electrical properties, J. Mater. Chem. 22 (2012), 22881. https://doi.org/10.1039/c2jm35064e.
[34] M. Prezioso, F.M. Bayat, B. Hoskins, K. Likharev, D. Strukov, Self-adaptive spike-time-dependent plasticity of metal-oxide memristors, Sci Rep 6 (2016)https://doi.org/10.1038/srep21331.